Journal of Molecular Catalysis A: Chemical 336 (2011) 78–86

Contents lists available at ScienceDirect

Journal of Molecular Catalysis A: Chemical

journal homepage: www.elsevier.com/locate/molcata

Direct synthesis of hydrogen peroxide from hydrogen and oxygen over palladium catalyst supported on $H_3PW_{12}O_{40}$-incorporated MCF silica

Sunyoung Park [a], Dong Ryul Park [a], Jung Ho Choi [a], Tae Jin Kim [b], Young-Min Chung [b], Seung-Hoon Oh [b], In Kyu Song [a,*]

[a] *School of Chemical and Biological Engineering, Institute of Chemical Processes, Seoul National University, Shinlim-dong, Kwanak-ku, Seoul 151-744, South Korea*
[b] *SK Energy Corporation, Yuseong-ku, Daejeon 305-712, South Korea*

ARTICLE INFO

Article history:
Received 30 September 2010
Received in revised form
17 December 2010
Accepted 21 December 2010
Available online 12 January 2011

Keywords:
Hydrogen peroxide
Palladium
Heteropolyacid
MCF silica

ABSTRACT

Palladium catalysts supported on $H_3PW_{12}O_{40}$ heteropolyacid incorporated into MCF silica (Pd/HPW-MCF-*X* (*X* = 1.0, 4.8, 9.1, 13.0, 16.7, 20.0, 23.1, and 25.9)) were prepared with a variation of $H_3PW_{12}O_{40}$ content (*X*, wt.%). The prepared catalysts were then applied to the direct synthesis of hydrogen peroxide from hydrogen and oxygen. Conversion of hydrogen over Pd/HPW-MCF-*X* catalysts showed no great difference, while selectivity for hydrogen peroxide and yield for hydrogen peroxide over the catalysts showed volcano-shaped curves with respect to $H_3PW_{12}O_{40}$ content. Acidity of Pd/HPW-MCF-*X* catalysts also showed a volcano-shaped trend with respect to $H_3PW_{12}O_{40}$ content. It was observed that yield for hydrogen peroxide increased with increasing acidity of Pd/HPW-MCF-*X* catalyst. Thus, acidity of Pd/HPW-MCF-*X* catalyst played an important role in determining the catalytic performance in the direct synthesis of hydrogen peroxide. HPW-MCF-*X* support efficiently served as an alternate acid source in the direct synthesis of hydrogen peroxide.

1. Introduction

Hydrogen peroxide (H_2O_2) has been widely used as a clean and strong oxidant in pulp industry, textile industry, and green chemical synthesis such as epoxidation of olefins and hydroxylation of benzene [1–4]. Hydrogen peroxide currently available in the industrial market is mostly produced through the anthraquinone auto-oxidation process [1,2]. However, this process uses toxic compounds and requires many energy intensive steps for separation and purification of hydrogen peroxide [1,2]. Therefore, direct synthesis of hydrogen peroxide from hydrogen and oxygen has attracted much attention as an economical and environmentally benign process [5–21].

In the direct synthesis of hydrogen peroxide from hydrogen and oxygen, several undesired reactions occur simultaneously together with selective oxidation of hydrogen to hydrogen peroxide ($H_2 + O_2 \rightarrow H_2O_2$, $\Delta H^\circ_{298\,K} = -135.8$ kJ/mol, $\Delta G^\circ_{298\,K} = -120.4$ kJ/mol) [2]. These undesired reactions include formation of water ($H_2 + 0.5O_2 \rightarrow H_2O$, $\Delta H^\circ_{298\,K} = -241.6$ kJ/mol, $\Delta G^\circ_{298\,K} = -237.2$ kJ/mol), hydrogenation of hydrogen peroxide ($H_2O_2 + H_2 \rightarrow 2H_2O$, $\Delta H^\circ_{298\,K} = -211.5$ kJ/mol, $\Delta G^\circ_{298\,K} = -354.0$ kJ/mol), and decomposition of hydrogen peroxide ($H_2O_2 \rightarrow H_2O + 0.5O_2$, $\Delta H^\circ_{298\,K} = -105.8$ kJ/mol, $\Delta G^\circ_{298\,K} = -116.8$ kJ/mol) [2]. All these reactions are thermodynamically favorable and highly exothermic. In particular, formation of water and hydrogenation of hydrogen peroxide are thermodynamically more favorable than selective oxidation of hydrogen to hydrogen peroxide. Consequently, selectivity for hydrogen peroxide in the direct synthesis of hydrogen peroxide is limited by these undesired reactions. Therefore, many attempts have been made to increase the selectivity for hydrogen peroxide in the direct synthesis of hydrogen peroxide [9–13].

Various noble metals such as palladium [5–13], palladium–gold [14–16], and palladium–platinum [17] are known to be efficient catalysts in the direct synthesis of hydrogen peroxide from hydrogen and oxygen. These noble metals have been supported on various materials such as silica, alumina, titania, zirconia, and carbon for effective dispersion of active metal component [8–17].

Acids and halides have been used as additives to enhance the selectivity for hydrogen peroxide in the direct synthesis of hydrogen peroxide from hydrogen and oxygen [1,2,9–13]. It has been reported that acids prevent the decomposition of hydrogen peroxide and halides inhibit the formation of water [1,2,9–13]. However, acid additives cause the corrosion of reactor as well as the dissolution of active metal component from the supported catalyst. Therefore, solid acid supports have been investigated in the direct

---

[*] Corresponding author. Tel.: +82 2 880 9227; fax: +82 2 889 7415.
E-mail address: inksong@snu.ac.kr (I.K. Song).

1381-1169/$ – see front matter © 2011 Elsevier B.V. All rights reserved.
doi:10.1016/j.molcata.2010.12.012

synthesis of hydrogen peroxide as an alternate acid source [18–21].

Heteropolyacids (HPAs) are inorganic acids. It has been reported that acid strength of HPAs is stronger than that of conventional solid acids [22–27]. Therefore, HPAs have been utilized as solid acid catalysts in several acid-catalyzed reactions [22,23]. However, HPAs are highly soluble in polar solvents and have low surface area (<10 m^2/g) [22]. In order to solve these problems, insoluble HPAs have been prepared by exchanging protons with certain cations [26,27]. It has been reported that HPA salts with large cations such as NH_4^+, K^+, Rb^+, and Cs^+ are insoluble, and have high surface area (>100 m^2/g) and porous structure by forming a tertiary structure [26,27]. In our previous work [20], palladium-exchanged insoluble HPA catalysts showed high catalytic performance in the direct synthesis of hydrogen peroxide from hydrogen and oxygen. However, it was difficult to separate palladium-exchanged insoluble HPA catalyst from reaction medium because insoluble HPA was composed of very fine particles with an average size of ca. 10 nm [26,27]. To overcome this problem, insoluble HPAs have been supported on porous materials such as zeolites and mesoporous silicas [21,28,29].

Mesoporous silicas have uniform pore size, high surface area, and large pore volume. Therefore, they have been used in many areas of science and engineering such as catalysis, adsorption, and separation [30–33]. Especially, it has been reported that mesostructured cellular foam (MCF) silica exhibits a 3-dimensional pore structure with large pores in the range of 10–50 nm [31–33]. Due to its unique pore characteristics, MCF silica has been used as an efficient support for immobilization of large molecules such as enzymes [33]. In our previous work [21], it was observed that insoluble $Cs_{2.5}H_{0.5}PW_{12}O_{40}$ heteropolyacid supported on Pd/MCF catalyst showed high catalytic performance in the direct synthesis of hydrogen peroxide from hydrogen and oxygen. However, insoluble $Cs_{2.5}H_{0.5}PW_{12}O_{40}$ heteropolyacid supported on Pd/MCF catalyst required many preparation steps.

In this work, a series of $H_3PW_{12}O_{40}$ heteropolyacid incorporated into MCF silica ($H_3PW_{12}O_{40}$-MCF) were prepared with a variation of $H_3PW_{12}O_{40}$ content for use as a solid acid support. Palladium catalysts supported on $H_3PW_{12}O_{40}$ heteropolyacid incorporated into MCF silica (Pd/$H_3PW_{12}O_{40}$-MCF) were then applied to the direct synthesis of hydrogen peroxide from hydrogen and oxygen. The effect of $H_3PW_{12}O_{40}$ content on the catalytic performance of Pd/$H_3PW_{12}O_{40}$-MCF catalysts in the direct synthesis of hydrogen peroxide was examined. A correlation between acidity and catalytic performance of Pd/$H_3PW_{12}O_{40}$-MCF catalysts was then established.

2. Experimental

2.1. Catalyst preparation

A series of $H_3PW_{12}O_{40}$ heteropolyacid incorporated into MCF silica ($H_3PW_{12}O_{40}$-MCF) were prepared with a variation of $H_3PW_{12}O_{40}$ content. Palladium catalysts supported on $H_3PW_{12}O_{40}$ heteropolyacid incorporated into MCF silica (Pd/$H_3PW_{12}O_{40}$-MCF) were then prepared by an incipient wetness impregnation method.

Typical procedures for the preparation of Pd/$H_3PW_{12}O_{40}$-MCF catalyst are as follows. 10 g of PEO-PPO-PEO triblock copolymer (Pluronic P123, BASF), an organic template, was dissolved in 350 ml of 1.6 M HCl aqueous solution at 40 °C. 25 ml of $H_3PW_{12}O_{40}$ (HPW) (Sigma–Aldrich) aqueous solution was added dropwise into the solution under vigorous stirring, and the mixed solution was stirred for 6 h. 4.6 ml of 1,3,5-trimethylbenzene (Mesitylene, Sigma–Aldrich), a swelling agent, was then added into the mixed solution. After stirring the solution at 40 °C for 1 h, 24.1 ml of tetraethyl orthosilicate (TEOS, Sigma–Aldrich), a silica source, was added into the solution. The resulting mixture was stirred at 40 °C for 20 h, and it was maintained at 130 °C for 20 h under static condition. After filtering and washing a solid product with distilled water, the solid was dried at room temperature. The solid product was then calcined in air at 500 °C for 5 h to yield $H_3PW_{12}O_{40}$-MCF support. Palladium nitrate ($Pd(NO_3)_2$, Sigma–Aldrich) was supported onto $H_3PW_{12}O_{40}$-MCF. The impregnated solid was dried overnight at 80 °C, and calcined at 500 °C for 3 h. The palladium loading was fixed at 0.5 wt.%. The calcined catalyst was charged into a tubular quartz reactor, and then it was reduced with a mixed stream of H_2 (5 ml/min) and N_2 (20 ml/min) at 200 °C for 2 h to yield Pd/$H_3PW_{12}O_{40}$-MCF catalyst. $H_3PW_{12}O_{40}$ content in the Pd/$H_3PW_{12}O_{40}$-MCF catalysts was adjusted to be 1.0, 4.8, 9.1, 13.0, 16.7, 20.0, 23.1, and 25.9 wt.%. Pd/$H_3PW_{12}O_{40}$-MCF catalysts were denoted as Pd/HPW-MCF-X (X = 1.0, 4.8, 9.1, 13.0, 16.7, 20.0, 23.1, and 25.9), where X represented weight percentage of $H_3PW_{12}O_{40}$ incorporated into MCF silica.

For comparison, palladium catalyst supported on MCF silica (Pd/MCF) was prepared by an incipient wetness method. MCF silica was synthesized according to the reported method [31]. The preparation procedures for Pd/MCF were almost identical to those for Pd/$H_3PW_{12}O_{40}$-MCF, except that $H_3PW_{12}O_{40}$ was not employed for the preparation of Pd/MCF. The palladium loading was also fixed at 0.5 wt.%.

2.2. Catalyst characterization

$H_3PW_{12}O_{40}$ content in the catalyst was measured by ICP-AES analysis (Shimadzu, ICPS-7500). Pore structure, pore size, and palladium dispersion of the catalyst were examined by TEM analysis (Jeol, JEM-3000F). N_2 adsorption–desorption isotherm of the catalyst was obtained with an ASAP-2010 instrument (Micromeritics), and pore size distribution was determined by the BJH (Barret–Joyner–Hallender) method applied to the desorption branch of the isotherm. X-ray diffraction (XRD) pattern of the catalyst was confirmed by XRD measurement (Rigaku, D-Max2500-PC) using CuKα radiation operated at 50 kV and 100 mA. Chemical state of $H_3PW_{12}O_{40}$ heteropolyacid incorporated into MCF silica was examined by ^{31}P MAS NMR analysis (Bruker, AVANCE 400 WB). NH_3-TPD (temperature-programmed desorption) experiment was carried out in order to measure the acidity of the catalyst. 0.05 g of each catalyst charged into the TPD apparatus was pretreated at 200 °C for 1 h with a stream of helium (20 ml/min). After cooling the catalyst to room temperature, 20 ml of NH_3 was pulsed into the reactor every minute under a flow of helium (5 ml/min) until the acid sites were saturated with NH_3. Physisorbed NH_3 was removed by evacuating the catalyst sample at 100 °C for 1 h. Furnace temperature was then increased from room temperature to 900 °C at a heating rate of 5 °C/min under a flow of helium (10 ml/min). Desorbed NH_3 was detected using a GC-MSD (Agilent, MSD-6890N GC).

2.3. Direct synthesis of hydrogen peroxide

Direct synthesis of hydrogen peroxide from hydrogen and oxygen was carried out in an autoclave reactor in the absence of acid additive. 80 ml of methanol and 6.32 mg of sodium bromide were charged into the reactor. 1 g of each catalyst was then added into the reactor. H_2/N_2 (25 mol% H_2) and O_2/N_2 (50 mol% O_2) were bubbled through the reaction medium under vigorous stirring (1000 rpm). H_2/O_2 ratio in the feed stream was fixed at 0.4, and total feed rate was maintained at 44 ml/min. Catalytic reaction was carried out at 28 °C and 10 atm for 6 h. In the catalytic reaction, mixed gases diluted with an inert gas (H_2/N_2 (25 mol% H_2) and O_2/N_2 (50 mol% O_2)) and an autoclave reactor equipped with a flashback arrestor as well as a safety valve were used in order to solve the safety

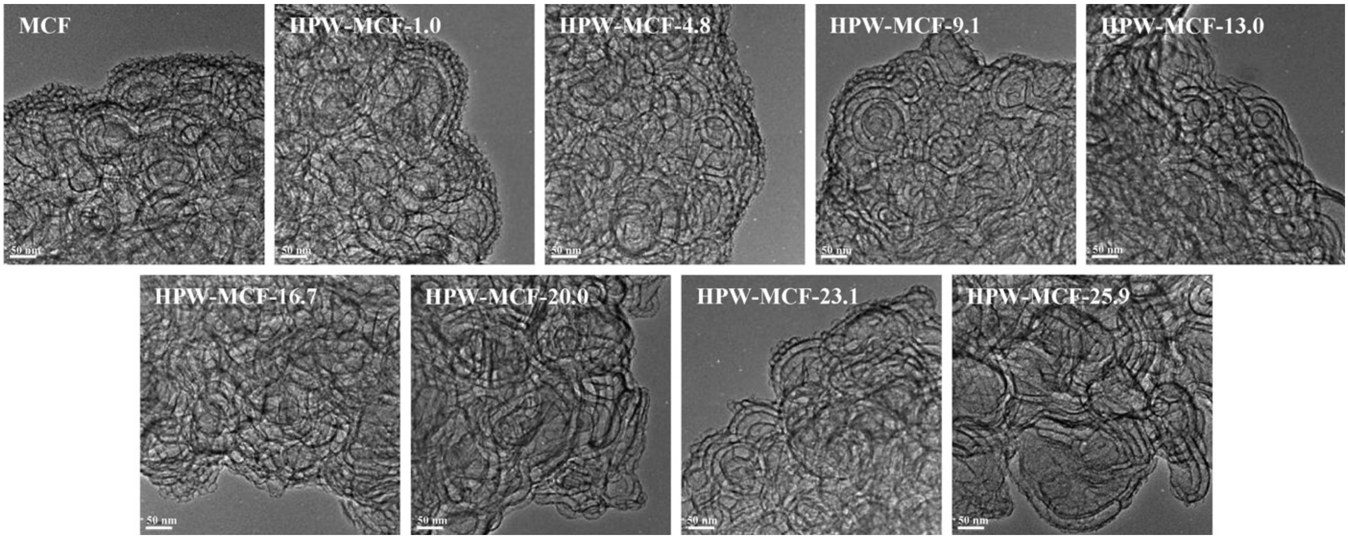

Fig. 1. TEM images of MCF silica and HPW-MCF-*X* (*X* = 1.0, 4.8, 9.1, 13.0, 16.7, 20.0, 23.1, and 25.9) supports.

problem. Unreacted hydrogen was analyzed using a gas chromatograph (Younglin, ACME 6000) equipped with a TCD. Concentration of hydrogen peroxide was determined by an iodometric titration method [34]. Conversion of hydrogen and selectivity for hydrogen peroxide were calculated according to the following equations. Yield for hydrogen peroxide was calculated by multiplying conversion of hydrogen and selectivity for hydrogen peroxide.

$$\text{Conversion of hydrogen} = \frac{\text{moles of hydrogen reacted}}{\text{moles of hydrogen supplied}}$$

$$\text{Selectivity for hydrogen peroxide} = \frac{\text{moles of hydrogen peroxide formed}}{\text{moles of hydrogen reacted}}$$

2.4. Hydrogenation of hydrogen peroxide

80 ml of methanol, 6.32 mg of sodium bromide, and 1 g of Pd/HPW-MCF-20.0 catalyst were charged into the reactor. 3 ml of 30 wt.% hydrogen peroxide was then added. H_2/N_2 (25 mol% H_2) and N_2 were bubbled through the reaction medium under vigorous stirring (1000 rpm). H_2/N_2 ratio in the feed stream was fixed at 0.1, and total feed rate was maintained at 44 ml/min. The reaction was carried out at 28 °C and 10 atm for 6 h. Concentration of hydrogen peroxide was determined by an iodometric titration method [34]. Degree of hydrogenation of hydrogen peroxide was calculated according to the following equation. For comparison, hydrogenation of hydrogen peroxide was also carried out using 1 g of Pd/MCF under the same reaction conditions.

$$\text{Degree of hydrogenation of } H_2O_2 = \frac{\text{moles of hydrogen peroxide hydrogenated}}{\text{moles of hydrogen peroxide supplied}}$$

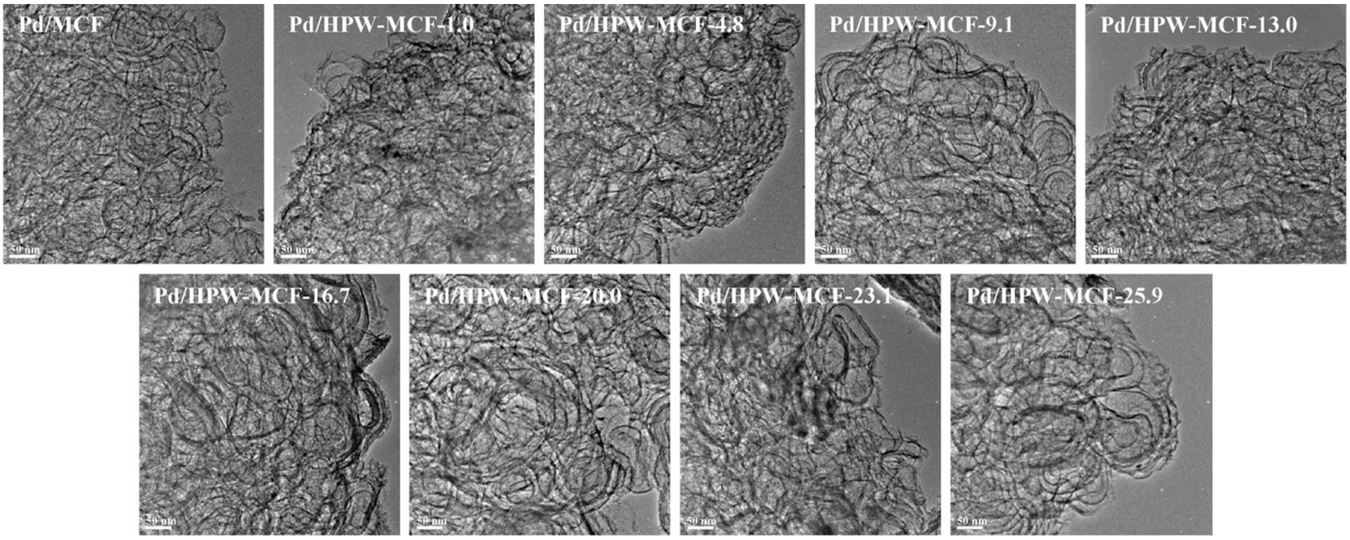

Fig. 2. TEM images of Pd/MCF and Pd/HPW-MCF-*X* (*X* = 1.0, 4.8, 9.1, 13.0, 16.7, 20.0, 23.1, and 25.9) catalysts.

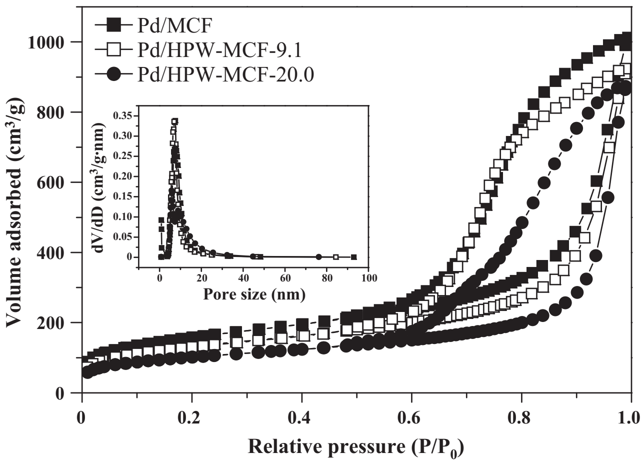

Fig. 3. N_2 adsorption–desorption isotherms and pore size distributions of Pd/MCF, Pd/HPW-MCF-9.1, and Pd/HPW-MCF-20.0.

2.5. Decomposition of hydrogen peroxide

80 ml of methanol, 6.32 mg of sodium bromide, and 1 g of Pd/HPW-MCF-20.0 catalyst were charged into the reactor. 3 ml of 30 wt.% hydrogen peroxide was then added. N_2 (44 ml/min) was bubbled through the reaction medium under vigorous stirring (1000 rpm). The reaction was carried out at 28 °C and 10 atm for 6 h. Concentration of hydrogen peroxide was determined by an iodometric titration method [34]. Degree of decomposition of hydrogen peroxide was calculated according to the following equation. For comparison, decomposition of hydrogen peroxide was also carried out using 1 g of Pd/MCF under the same reaction conditions.

$$\text{Degree of decomposition of } H_2O_2 = \frac{\text{moles of hydrogen peroxide decomposed}}{\text{moles of hydrogen peroxide supplied}}$$

3. Results and discussion

3.1. Catalyst characterization

$H_3PW_{12}O_{40}$ (HPW) content in the Pd/HPW-MCF-*X* (*X* = 1.0, 4.8, 9.1, 13.0, 16.7, 20.0, 23.1, and 25.9) catalysts determined by ICP-AES analyses is listed in Table 1. $H_3PW_{12}O_{40}$ content in the Pd/HPW-MCF-*X* catalysts increased with increasing designed value. This indicates that Pd/HPW-MCF-*X* catalysts were successfully prepared as attempted in this work.

Fig. 1 shows the TEM images of MCF and HPW-MCF-*X* (*X* = 1.0, 4.8, 9.1, 13.0, 16.7, 20.0, 23.1, and 25.9) supports. Pore structure and pore size of HPW-MCF-*X* were almost identical to those of MCF silica. HPW-MCF-*X* exhibited a disordered pore structure with large pores in the range of 8–10 nm. This indicates that HPW-MCF-*X* supports were successfully prepared and pore structure of MCF silica was still maintained even after the incorporation of $H_3PW_{12}O_{40}$.

Fig. 2 shows the TEM images of Pd/MCF and Pd/HPW-MCF-*X* (*X* = 1.0, 4.8, 9.1, 13.0, 16.7, 20.0, 23.1, and 25.9) catalysts. Pd/HPW-MCF-*X* catalysts exhibited almost the same pore structure and pore size as HPW-MCF-*X* supports, indicating that pore structure of the supports was still maintained even after the palladium loading. Furthermore, small palladium particles with a size of 10–40 nm were observed in the TEM images of the catalysts. Palladium dispersion determined by hydrogen chemisorption was in the range of 2.7–7.9%.

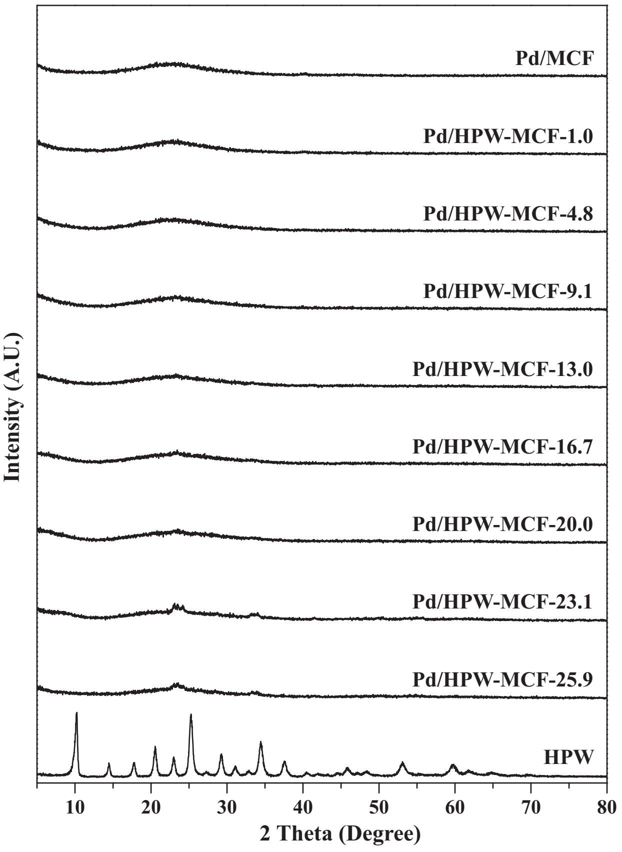

Fig. 4. XRD patterns of Pd/MCF, $H_3PW_{12}O_{40}$ (HPW), and Pd/HPW-MCF-*X* (*X* = 1.0, 4.8, 9.1, 13.0, 16.7, 20.0, 23.1, and 25.9) catalysts.

Fig. 3 shows the N_2 adsorption–desorption isotherms and pore size distributions of Pd/MCF, Pd/HPW-MCF-9.1, and Pd/HPW-MCF-20.0. N_2 adsorption–desorption isotherm and pore size distribution of Pd/HPW-MCF-*X* catalysts were similar to those of Pd/MCF. Pd/HPW-MCF-*X* catalysts showed IV-type isotherms with H1-type hysteresis loops, as reported in the literature [31]. This result also supports that pore structure of MCF silica was still maintained even after the incorporation of $H_3PW_{12}O_{40}$ and the loading of palladium, as also evidenced by TEM images. Detailed textural properties of Pd/HPW-MCF-*X* catalysts are summarized in Table 1. Surface area of Pd/HPW-MCF-*X* catalysts decreased with increasing $H_3PW_{12}O_{40}$ content. This is attributed to the increased incorporation of $H_3PW_{12}O_{40}$ into MCF silica. Pore volume of Pd/HPW-MCF-*X* catalysts also decreased with increasing $H_3PW_{12}O_{40}$ content. Furthermore, it was observed that average pore size of Pd/HPW-MCF-*X* catalysts slightly increased with increasing $H_3PW_{12}O_{40}$ content. However, all the Pd/HPW-MCF-*X* catalysts still exhibited the unique pore characteristics of MCF silica.

Fig. 4 shows the XRD patterns of Pd/MCF, $H_3PW_{12}O_{40}$ (HPW), and Pd/HPW-MCF-*X* (*X* = 1.0, 4.8, 9.1, 13.0, 16.7, 20.0, 23.1, and 25.9) catalysts. Pd/MCF showed no diffraction peaks due to an amorphous nature of MCF silica [32]. No diffraction peaks for $H_3PW_{12}O_{40}$ were also observed in the Pd/HPW-MCF-*X* (*X* = 1.0, 4.8, 9.1, 13.0, 16.7, and 20.0) catalysts. This indicates that $H_3PW_{12}O_{40}$ was not in a crystal state but in an amorphous-like state, demonstrating that $H_3PW_{12}O_{40}$ was finely and molecularly incorporated into MCF silica. However, Pd/HPW-MCF-23.1 and Pd/HPW-MCF-25.9 catalysts exhibited weak diffraction peaks for $H_3PW_{12}O_{40}$. This implies that $H_3PW_{12}O_{40}$ was aggregated by the excessive incorporation of $H_3PW_{12}O_{40}$ into MCF silica.

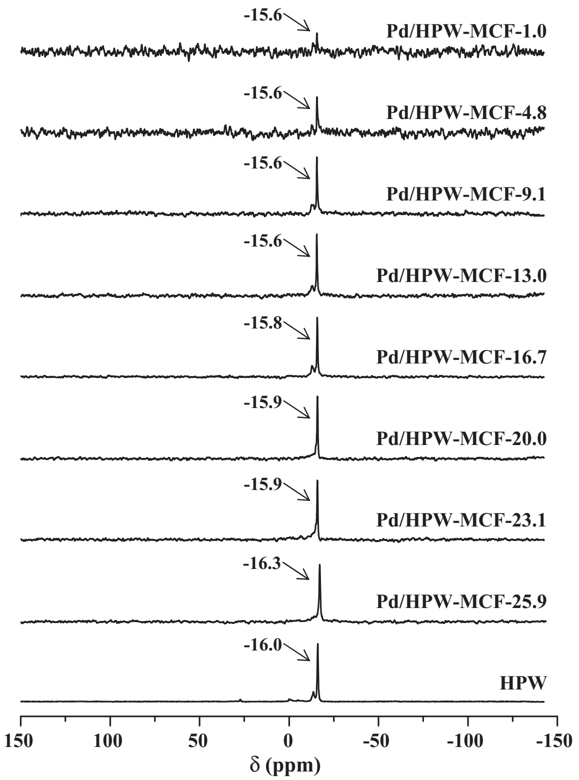

Fig. 5. ^{31}P MAS NMR spectra of $H_3PW_{12}O_{40}$ (HPW) and Pd/HPW-MCF-X (X = 1.0, 4.8, 9.1, 13.0, 16.7, 20.0, 23.1, and 25.9) catalysts.

Fig. 5 shows the ^{31}P MAS NMR spectra of $H_3PW_{12}O_{40}$ (HPW) and Pd/HPW-MCF-X (X = 1.0, 4.8, 9.1, 13.0, 16.7, 20.0, 23.1, and 25.9) catalysts. It has been reported that $H_3PW_{12}O_{40}$ exhibited a resonance peak at around −15 or −16 ppm [35–37]. It is known that small difference in chemical shift was attributed to the difference in the degree of hydration [35,36]. All the Pd/HPW-MCF-X catalysts showed a resonance peak in the range from −15.6 to −16.3 ppm. This chemical shift was similar to that of $H_3PW_{12}O_{40}$ (−16.0 ppm), indicating that the chemical interaction between $H_3PW_{12}O_{40}$ and MCF silica in Pd/HPW-MCF-X catalysts was negligible. Therefore, it is expected that $H_3PW_{12}O_{40}$ was incorporated into MCF silica by being embedded in the silica framework. Furthermore, any peaks were not detected at −30 ppm. This implies that no phosphorous oxide was formed under our preparation conditions [37]. This result indicates that the primary structure of $H_3PW_{12}O_{40}$ was still maintained even after the incorporation into MCF silica.

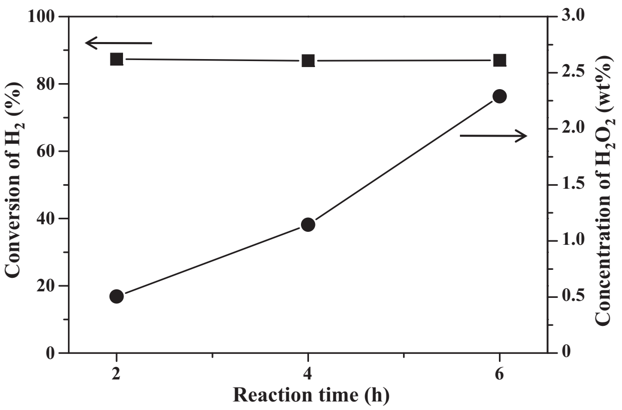

Fig. 6. Catalytic performance of Pd/HPW-MCF-20.0 catalyst in the direct synthesis of hydrogen peroxide from hydrogen and oxygen with time on stream.

3.2. Catalytic performance in the direct synthesis of hydrogen peroxide

Fig. 6 shows the catalytic performance of Pd/HPW-MCF-20.0 catalyst in the direct synthesis of hydrogen peroxide from hydrogen and oxygen with time on stream. Conversion of hydrogen was almost constant during a 6 h-reaction, while concentration of hydrogen peroxide continuously increased with increasing reaction time. This indicates that the catalyst deactivation did not occur during the reaction extending over 6 h. Furthermore, it is expected that decomposition of hydrogen peroxide during the reaction was negligible.

Fig. 7 shows the catalytic performance of Pd/HPW-MCF-X (X = 1.0, 4.8, 9.1, 13.0, 16.7, 20.0, 23.1, and 25.9) catalysts in the direct synthesis of hydrogen peroxide from hydrogen and oxygen after a 6-h reaction, plotted as a function of $H_3PW_{12}O_{40}$ content. Conversion of hydrogen over the catalysts showed no great difference, while selectivity for hydrogen peroxide exhibited a volcano-shaped curve with respect to $H_3PW_{12}O_{40}$ content. As a consequence, yield for hydrogen peroxide showed a volcano-shaped curve with respect to $H_3PW_{12}O_{40}$ content. Final concentration of hydrogen peroxide after a 6 h-reaction also showed a volcano-shaped curve with respect to $H_3PW_{12}O_{40}$ content. Among the catalysts tested, Pd/HPW-MCF-20.0 catalyst showed the best catalytic performance in terms of selectivity for hydrogen peroxide, yield for hydrogen peroxide, and final concentration of hydrogen peroxide.

It is noteworthy that no significant dissolution of $H_3PW_{12}O_{40}$ was observed in the Pd/HPW-MCF-X (X = 1.0, 4.8, 9.1, 13.0, 16.7, 20.0, 23.1, and 25.9) catalysts before and after the direct synthesis of

Table 1
HPW content, surface area, pore volume, average pore size, and acidity of Pd/MCF and Pd/HPW-MCF-X catalysts.

Catalyst	HPW content (wt.%)		Surface area (m^2/g)[a]	Pore volume (cm^3/g)[b]	Average pore size (nm)[c]	Acidity (mmol-NH_3/g)
	Before reaction	After reaction				
Pd/MCF	–	–	561.8	1.6	8.0	26.4
Pd/HPW-MCF-1.0	0.7	0.7	538.1	1.6	8.3	106.3
Pd/HPW-MCF-4.8	4.8	4.4	524.1	1.4	7.1	130.0
Pd/HPW-MCF-9.1	7.5	6.5	468.0	1.4	8.0	131.7
Pd/HPW-MCF-13.0	10.0	8.7	403.0	1.5	8.8	156.6
Pd/HPW-MCF-16.7	12.1	10.1	365.4	1.5	8.9	161.8
Pd/HPW-MCF-20.0	17.2	14.4	358.1	1.4	9.8	170.9
Pd/HPW-MCF-23.1	17.5	15.8	348.2	1.1	9.6	167.7
Pd/HPW-MCF-25.9	22.8	17.9	347.7	1.1	9.2	127.2

[a] Calculated by the BET (Brunauer–Emmett–Teller) equation.
[b] BJH (Barret–Joyner–Hallender) desorption pore volume.
[c] BJH (Barret–Joyner–Hallender) desorption average pore diameter.

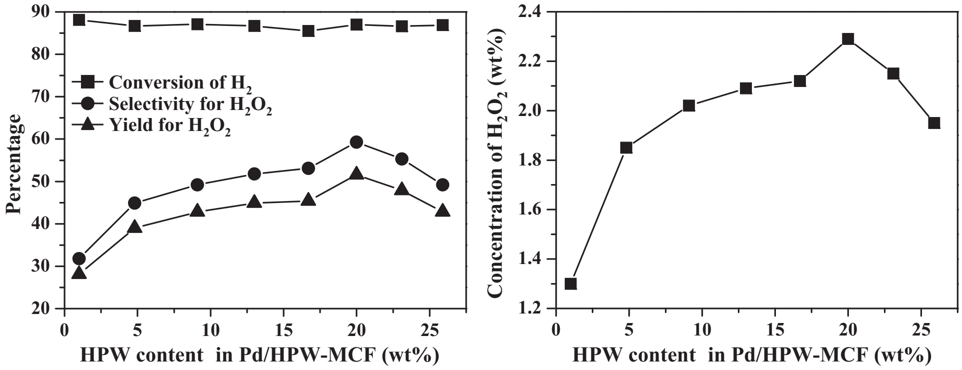

Fig. 7. Catalytic performance of Pd/HPW-MCF-*X* (*X* = 1.0, 4.8, 9.1, 13.0, 16.7, 20.0, 23.1, and 25.9) catalysts in the direct synthesis of hydrogen peroxide from hydrogen and oxygen after a 6 h-reaction.

hydrogen peroxide from hydrogen and oxygen, as listed in Table 1. This indicates that $H_3PW_{12}O_{40}$ was well incorporated into the pores of MCF silica, as attempted in this work.

Direct comparison of catalytic performance of Pd/HPW-MCF-20.0 with that of $Pd_{0.15}Cs_{2.5}H_{0.2}PW_{12}O_{40}$ (the optimum palladium-exchanged insoluble HPA catalyst in the literature [20]) revealed that yield for hydrogen peroxide over Pd/HPW-MCF-20.0 catalyst (51.6%) was higher than that over $Pd_{0.15}Cs_{2.5}H_{0.2}PW_{12}O_{40}$ catalyst (40.3%). Final concentration of hydrogen peroxide after a 6 h-reaction over Pd/HPW-MCF-20.0 catalyst (2.29 wt.%) was also higher than that over $Pd_{0.15}Cs_{2.5}H_{0.2}PW_{12}O_{40}$ catalyst (1.77 wt.%).

For comparison, Pd/MCF was applied to the direct synthesis of hydrogen peroxide from hydrogen and oxygen. Fig. 8 shows the catalytic performance of Pd/MCF and Pd/HPW-MCF-20.0 in the direct synthesis of hydrogen peroxide. Conversion of hydrogen over Pd/HPW-MCF-20.0 catalyst was almost identical to that over Pd/MCF, while selectivity for hydrogen peroxide over Pd/HPW-MCF-20.0 catalyst was much higher than that over Pd/MCF. Consequently, yield for hydrogen peroxide over Pd/HPW-MCF-20.0 catalyst was much higher than that over Pd/MCF. Final concentration of hydrogen peroxide after a 6 h-reaction over Pd/HPW-MCF-20.0 catalyst was also much higher than that over Pd/MCF. It has been reported that acid additives increase the selectivity for hydrogen peroxide by preventing the decomposition of hydrogen peroxide, because acid additives inhibited the dissociation of hydrogen peroxide ($H_2O_2 \Leftrightarrow HO_2^- + H^+$) by surrounding hydrogen peroxide with protons [2]. Therefore, it can be inferred that the improved selectivity for hydrogen peroxide over Pd/HPW-MCF-*X* (*X* = 1.0, 4.8, 9.1, 13.0, 16.7, 20.0, 23.1, and 25.9) catalysts was attributed to the enhanced acid property of Pd/HPW-MCF-*X* catalysts.

3.3. Effect of acid additive on the catalytic performance

Fig. 9 shows the catalytic performance of Pd/HPW-MCF-20.0 catalyst in the direct synthesis of hydrogen peroxide from hydrogen and oxygen at different concentration of H_3PO_4. 0.645 ml of 1 M H_3PO_4 solution was added to the reaction medium in order to make the concentration of H_3PO_4 become 1000 ppm. Conversion of hydrogen and selectivity for hydrogen peroxide in the presence of H_3PO_4 were almost identical to those in the absence of H_3PO_4. Consequently, yield for hydrogen peroxide in the presence of H_3PO_4 was similar to that in the absence of H_3PO_4. Final concentration of hydrogen peroxide in the presence of H_3PO_4 after a 6 h-reaction was also almost identical to that in the absence of H_3PO_4. This indicates that H_3PO_4 additive had no effect on the catalytic performance of Pd/HPW-MCF-20.0 catalyst.

Fig. 10 shows the catalytic performance of Pd/MCF in the direct synthesis of hydrogen peroxide from hydrogen and oxygen at different concentration of H_3PO_4. Conversion of hydrogen in the presence of H_3PO_4 was similar to that in the absence of H_3PO_4, while selectivity for hydrogen peroxide in the presence of H_3PO_4 was much higher than that in the absence of H_3PO_4. Consequently, yield for hydrogen peroxide in the presence of H_3PO_4 was considerably higher than that in the absence of H_3PO_4. Final concentration of hydrogen peroxide in the presence of H_3PO_4 after a 6 h-reaction was also much higher than that in the absence of H_3PO_4. This is in good agreement with the fact that acid additives enhanced the selectivity for hydrogen peroxide by preventing the decomposition of hydrogen peroxide [2].

Direct comparison of Figs. 9 and 10 revealed that the catalytic performance of Pd/MCF was more sensitive to the amount of H_3PO_4 additive than that of Pd/HPW-MCF-20.0 catalyst. Furthermore, the catalytic performance of Pd/HPW-MCF-20.0 catalyst even in the absence of H_3PO_4 was much higher than that of Pd/MCF in the presence of H_3PO_4. This result implies that $H_3PW_{12}O_{40}$-incorporated MCF silica served as an efficient alternate acid source in the direct synthesis of hydrogen peroxide from hydrogen and oxygen.

3.4. Catalytic performance in the hydrogenation of hydrogen peroxide and the decomposition of hydrogen peroxide

Fig. 11 shows the catalytic performance in the hydrogenation of hydrogen peroxide and the decomposition of hydrogen peroxide over Pd/MCF and Pd/HPW-MCF-20.0. Both Pd/MCF and Pd/HPW-MCF-20.0 showed high activity for hydrogenation of hydrogen peroxide. This indicates that the enhanced acid property of Pd/HPW-MCF-20.0 catalyst showed no significant effect on the prevention of hydrogenation of hydrogen peroxide. However, activity for decomposition of hydrogen peroxide over Pd/HPW-MCF-20.0 catalyst was much lower than that over Pd/MCF. This implies that the enhanced acid property of Pd/HPW-MCF-20.0 catalyst inhibited the decomposition of hydrogen peroxide. Therefore, it can be said that Pd/HPW-MCF-*X* (*X* = 1.0, 4.8, 9.1, 13.0, 16.7, 20.0, 23.1, and 25.9) catalysts increased the selectivity for hydrogen peroxide by preventing the decomposition of hydrogen peroxide.

3.5. Acidity of Pd/$H_3PW_{12}O_{40}$-MCF catalysts

Fig. 12 shows the NH_3-TPD profiles of Pd/MCF and Pd/HPW-MCF-*X* (*X* = 1.0, 4.8, 9.1, 13.0, 16.7, 20.0, 23.1, and 25.9) catalysts. Acidity of Pd/HPW-MCF-*X* catalysts measured from the peak area is summarized in Table 1. Acidity of the catalysts showed a volcano-shaped trend with respect to $H_3PW_{12}O_{40}$ content. Among the Pd/HPW-MCF-*X*-*X* catalysts, Pd/HPW-MCF-20.0 showed the largest acidity. It has been reported that acidity of $H_3PW_{12}O_{40}$-SBA-15 did not increase in proportion to $H_3PW_{12}O_{40}$ content, because $H_3PW_{12}O_{40}$ was covered with SBA-15 silica walls [37]. In this

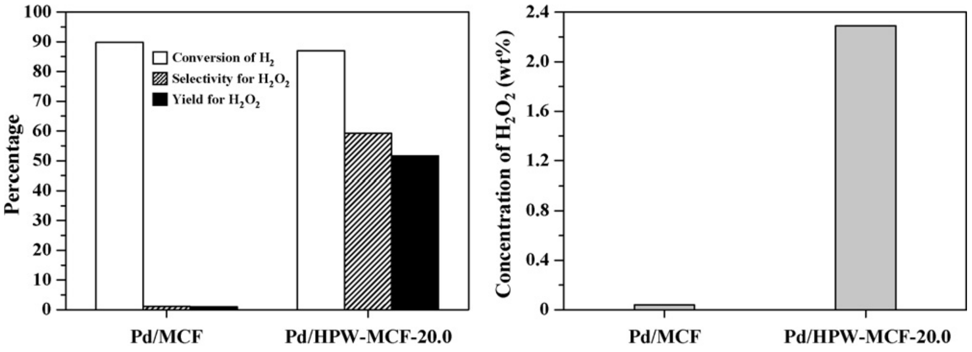

Fig. 8. Catalytic performance of Pd/MCF and Pd/HPW-MCF-20.0 in the direct synthesis of hydrogen peroxide from hydrogen and oxygen after a 6 h-reaction.

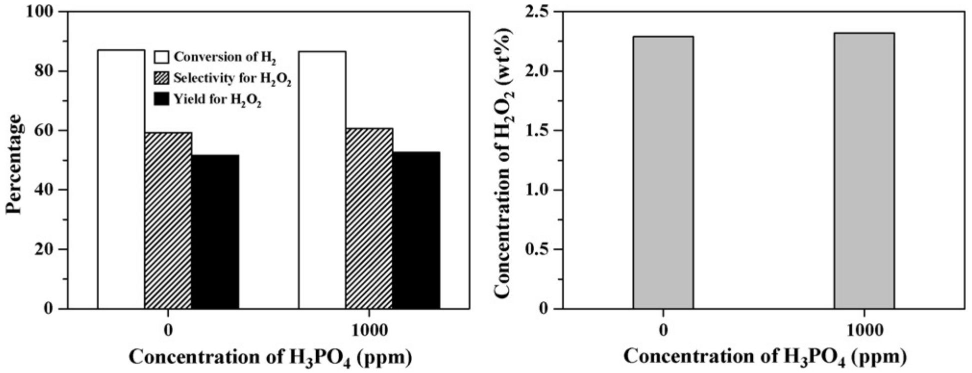

Fig. 9. Catalytic performance of Pd/HPW-MCF-20.0 catalyst in the direct synthesis of hydrogen peroxide from hydrogen and oxygen after a 6 h-reaction at different concentration of H_3PO_4.

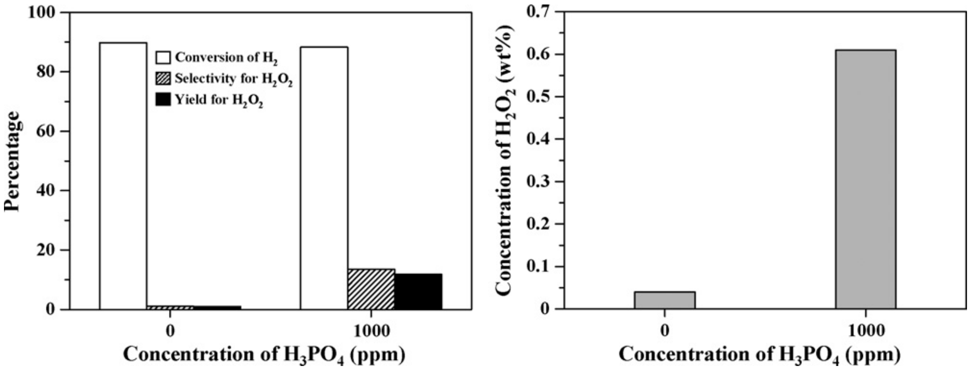

Fig. 10. Catalytic performance of Pd/MCF in the direct synthesis of hydrogen peroxide from hydrogen and oxygen after a 6 h-reaction at different concentration of H_3PO_4.

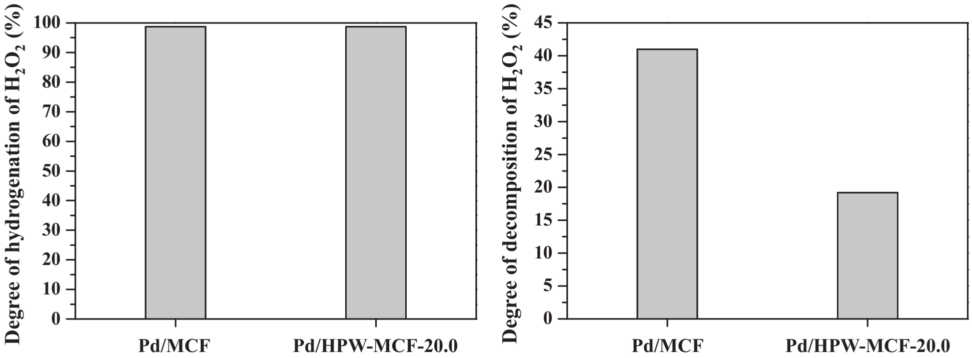

Fig. 11. Catalytic performance in the hydrogenation of hydrogen peroxide and the decomposition of hydrogen peroxide over Pd/MCF and Pd/HPW-MCF-20.0.

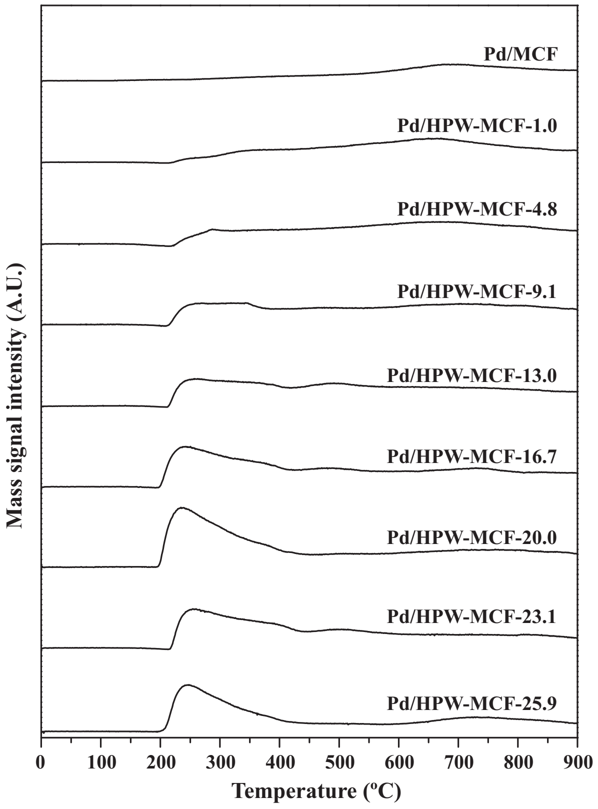

Fig. 12. NH_3-TPD profiles of Pd/MCF and Pd/HPW-MCF-*X* (*X* = 1.0, 4.8, 9.1, 13.0, 16.7, 20.0, 23.1, and 25.9) catalysts.

work, the aggregation of $H_3PW_{12}O_{40}$ was observed, when a large amount of $H_3PW_{12}O_{40}$ was added into MCF silica during the preparation step. Therefore, it can be inferred that the amount of $H_3PW_{12}O_{40}$ exposed on the surface of $H_3PW_{12}O_{40}$-incorporated MCF silica decreased because $H_3PW_{12}O_{40}$ agglomerates were caged in the silica framework, when a large amount of $H_3PW_{12}O_{40}$ was incorporated into MCF silica. This result indicates that acidity of Pd/HPW-MCF-*X* decreased due to the restriction of effective exposure of $H_3PW_{12}O_{40}$, when an excess amount of $H_3PW_{12}O_{40}$ more than 20.0 wt.% was employed for incorporation.

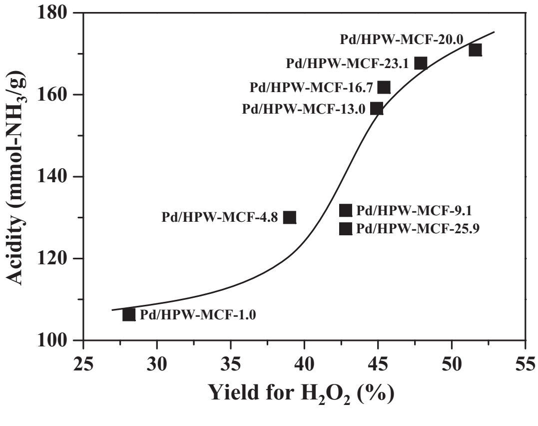

Fig. 13. A correlation between yield for hydrogen peroxide over Pd/HPW-MCF-*X* (*X* = 1.0, 4.8, 9.1, 13.0, 16.7, 20.0, 23.1, and 25.9) catalysts and acidity of the catalysts.

3.6. Effect of acidity on the catalytic performance

Fig. 13 shows the correlation between yield for hydrogen peroxide and acidity of Pd/HPW-MCF-*X* (*X* = 1.0, 4.8, 9.1, 13.0, 16.7, 20.0, 23.1, and 25.9) catalysts. The correlation clearly shows that yield for hydrogen peroxide over Pd/HPW-MCF-*X* catalysts was closely related to the acidity of the catalysts. Yield for hydrogen peroxide increased with increasing acidity of Pd/HPW-MCF-*X* catalyst. Among the catalysts tested, Pd/HPW-MCF-20.0 catalyst with the largest acidity showed the highest yield for hydrogen peroxide. It has been reported that acidity on the surface of the catalyst is an important factor determining the catalytic performance in the direct synthesis of hydrogen peroxide from hydrogen and oxygen [19–21]. Therefore, it is concluded that the improved yield for hydrogen peroxide over Pd/HPW-MCF-*X* catalysts was attributed to the enhanced acidity of the catalysts. Thus, Pd/HPW-MCF-*X* efficiently served as an alternate acid source and as an active metal catalyst in the direct synthesis of hydrogen peroxide.

4. Conclusions

A series of $H_3PW_{12}O_{40}$ heteropolyacid incorporated into MCF silica (HPW-MCF-*X* (*X* = 1.0, 4.8, 9.1, 13.0, 16.7, 20.0, 23.1, and 25.9)) were prepared with a variation of $H_3PW_{12}O_{40}$ content (*X*, wt.%). Palladium catalysts supported on $H_3PW_{12}O_{40}$-incorporated MCF silica (Pd/HPW-MCF-*X* (*X* = 1.0, 4.8, 9.1, 13.0, 16.7, 20.0, 23.1, and 25.9)) were then prepared for use in the direct synthesis of hydrogen peroxide from hydrogen and oxygen. High catalytic performance of Pd/HPW-MCF-*X* catalysts compared to Pd/MCF was attributed to the enhanced acid property of Pd/HPW-MCF-*X* catalysts. Conversion of hydrogen over Pd/HPW-MCF-*X* catalysts showed no great difference, while selectivity for hydrogen peroxide, yield for hydrogen peroxide, and final concentration of hydrogen peroxide over the catalysts showed volcano-shaped curves with respect to $H_3PW_{12}O_{40}$ content. Acidity of the catalysts also showed a volcano-shaped trend with respect to $H_3PW_{12}O_{40}$ content. It was revealed that yield for hydrogen peroxide increased with increasing acidity of Pd/HPW-MCF-*X* catalyst. Among the catalysts tested, Pd/HPW-MCF-20.0 catalyst with the largest acidity showed the highest yield for hydrogen peroxide. It is concluded that acidity of Pd/HPW-MCF-*X* catalyst played a crucial role in determining the catalytic performance in the direct synthesis of hydrogen peroxide.

Acknowledgements

This work was financially supported by the grant from the Industrial Source Technology Development Programs (10033093) of the Ministry of Knowledge Economy (MKE) of Korea.

References

[1] J.M. Campos-Martin, G. Blanco-Brieva, J.L.G. Fierro, Angew. Chem. Int. Ed. 45 (2006) 6962–6984.
[2] C. Samanta, Appl. Catal. A 350 (2008) 133–149.
[3] S. Bordiga, A. Damin, F. Bonino, C. Lamberti, Top Organomet. Chem. 16 (2005) 37–68.
[4] S. Park, K.M. Cho, M.H. Youn, J.G. Seo, J.C. Jung, S.-H. Baeck, T.J. Kim, Y.-M. Chung, S.-H. Oh, I.K. Song, Catal. Commun. 9 (2008) 2485–2488.
[5] J.H. Lunsford, J. Catal. 216 (2003) 455–460.
[6] S. Chinta, J.H. Lunsford, J. Catal. 225 (2004) 249–255.
[7] R. Burch, P.R. Ellis, Appl. Catal. B 42 (2003) 203–211.
[8] V.R. Choudhary, C. Samanta, T.V. Choudhary, Appl. Catal. A 308 (2006) 128–133.
[9] Y.-F. Han, J.H. Lunsford, J. Catal. 230 (2005) 313–316.
[10] V.R. Choudhary, S.D. Sansare, A.G. Gaikwad, Catal. Lett. 84 (2002) 81–87.
[11] V.R. Choudhary, C. Samanta, J. Catal. 238 (2006) 28–38.
[12] C. Samanta, V.R. Choudhary, Catal. Commun. 8 (2007) 73–79.
[13] V.R. Choudhary, P. Jana, Appl. Catal. A 352 (2009) 35–42.
[14] J.K. Edwards, B.E. Solsona, P. Landon, A.F. Carley, A. Herzing, C.J. Kiely, G.J. Hutchings, J. Catal. 236 (2005) 69–79.

[15] J.K. Edwards, A. Thomas, A.F. Carley, A.A. Herzing, C.J. Kiely, G.J. Hutchings, Green Chem. 10 (2008) 388–394.
[16] J.K. Edwards, B. Solsona, E. Ntainjua, A.F. Carley, A.A. Herzing, C.J. Kiely, G.J. Hutchings, Science 323 (2009) 1037–1041.
[17] Q. Liu, J.C. Bauer, R.E. Schaak, J.H. Lunsford, Appl. Catal. A 339 (2008) 130–136.
[18] F. Menegazzo, P. Burti, M. Signoretto, M. Manzoli, S. Vankova, F. Boccuzzi, F. Pinna, G. Strukul, J. Catal. 257 (2008) 369–381.
[19] S. Park, S.-H. Baeck, T.J. Kim, Y.-M. Chung, S.-H. Oh, I.K. Song, J. Mol. Catal. A 319 (2010) 98–107.
[20] S. Park, S.H. Lee, S.H. Song, D.R. Park, S.-H. Baeck, T.J. Kim, Y.-M. Chung, S.-H. Oh, I.K. Song, Catal. Commun. 10 (2009) 391–394.
[21] S. Park, D.R. Park, J.H. Choi, T.J. Kim, Y.-M. Chung, S.-H. Oh, I.K. Song, J. Mol. Catal. A 332 (2010) 76–83.
[22] I.V. Kozhevnikov, Chem. Rev. 98 (1998) 171–198.
[23] C.L. Hill, C.M. Prosser-McCartha, Coord. Chem. Rev. 143 (1995) 407–455.
[24] I.K. Song, M.A. Barteau, Korean J. Chem. Eng. 19 (2002) 567–573.
[25] M.H. Youn, D.R. Park, J.C. Jung, H. Kim, M.A. Barteau, I.K. Song, Korean J. Chem. Eng. 24 (2007) 51–54.
[26] T. Okuhara, N. Mizuno, M. Misono, Adv. Catal. 41 (1996) 113–252.
[27] M. Misono, Chem. Commun. (2001) 1141–1152.
[28] F. Zhang, C. Yuan, J. Wang, Y. Kong, H. Zhu, C. Wang, J. Mol. Catal. A 247 (2006) 130–137.
[29] R. Gao, H. Chen, Y. Le, W.-L. Dai, K. Fan, Appl. Catal. A 352 (2009) 61–65.
[30] M. Thommes, R. Köhn, M. Fröba, Appl. Surf. Sci. 196 (2002) 239–249.
[31] P. Schmidt-Winkel, W.W. Lukens Jr., P. Yang, D.I. Margolese, J.S. Lettow, J.Y. Ying, G.D. Stucky, Chem. Mater. 12 (2000) 686–696.
[32] H. Kim, J.C. Jung, S.H. Yeom, K.-Y. Lee, J. Yi, I.K. Song, Mater. Res. Bull. 42 (2007) 2132–2142.
[33] K. Kannan, R.V. Jasra, J. Mol. Catal. B 56 (2009) 34–40.
[34] R.M. Hanson, K.B. Sharpless, J. Org. Chem. 51 (1986) 1922–1925.
[35] S. Damyanova, L. Dimitrov, R. Mariscal, J.L.G. Fierro, L. Petrov, I. Sobrados, Appl. Catal. A 256 (2003) 183–197.
[36] A. Ghanbari-Siahkali, A. Philippou, J. Dwyer, M.W. Anderson, Appl. Catal. A 192 (2000) 57–69.
[37] B.C. Gagea, Y. Lorgouilloux, Y. Altintas, P.A. Jacobs, J.A. Martens, J. Catal. 265 (2009) 99–108.